

# Viral and immune dynamics of HPV genital infections in young women

Nicolas Tessandier<sup>1,+</sup>, Baptiste Elie<sup>2,+</sup>, Vanina Boué<sup>2</sup>, Christian Selinger<sup>2,3</sup>,  
Massilva Rahmoun<sup>2</sup>, Claire Bernat<sup>2,4</sup>, Sophie Grasset<sup>2</sup>, Soraya Groc<sup>2,5</sup>,  
Anne-Sophie Bedin<sup>5</sup>, Thomas Beneteau<sup>2</sup>, Marine Bonneau<sup>6</sup>, Christelle Graf<sup>6</sup>,  
Nathalie Jacobs<sup>7</sup>, Tsukushi Kamiya<sup>1</sup>, Marion Keriou<sup>8</sup>, Julie Lajoie<sup>9</sup>,  
Imène Melki<sup>1</sup>, Jean-Luc Prétet<sup>10,11</sup>, Bastien Reyné<sup>2</sup>, Géraldine Schlecht-Louf<sup>12</sup>,  
Mircea T. Sofonea<sup>5,13</sup>, Olivier Supplisson<sup>1,14</sup>, Vincent Foulongne<sup>5</sup>, Jérémie Guedj<sup>8</sup>,  
Christophe Hirtz<sup>16</sup>, Marie-Christine Picot<sup>17</sup>, Jacques Reynes<sup>18</sup>, Vincent Tribut<sup>19</sup>,  
Édouard Tuillon<sup>5</sup>, Tim Waterboer<sup>20</sup>, Michel Segondy<sup>5</sup>, Ignacio G Bravo<sup>2</sup>,  
Nathalie Boule<sup>5</sup>, Carmen Lia Mural<sup>2,21</sup>, Samuel Alizon<sup>1,2,\*</sup>

<sup>1</sup> CIRB, CNRS, INSERM, Collège de France, Université PSL, Paris, France

<sup>2</sup> MIVEGEC, CNRS, IRD, Université de Montpellier, France

<sup>3</sup> Swiss Tropical and Public Health Institute, Basel, Switzerland

<sup>4</sup> CNRS UMR 5203, Institut de Génomique Fonctionnelle, Montpellier, France

<sup>5</sup> Pathogenesis and Control of Chronic Infections, INSERM, CHU, University of Montpellier, Montpellier, France

<sup>6</sup> Department of Obstetrics and Gynaecology, Centre Hospitalier Universitaire de Montpellier, Montpellier, France

<sup>7</sup> Laboratory of Cellular and Molecular Immunology, GIGA Research, University of Liège, 4000 Liège, Belgium

<sup>8</sup> INSERM, IAME, Université de Paris, Paris, France

<sup>9</sup> Department of Medical Microbiology, University of Manitoba, Winnipeg, Manitoba, Canada

<sup>10</sup> EA3181, UBFC, LabEx LipSTIC ANR-11-LABX-0021, Besançon, France

<sup>11</sup> Centre National de Référence Papillomavirus, CHRU de Besançon, Besançon, France

<sup>12</sup> UMR996, Inflammation, Chemokines and Immunopathology, INSERM, Université Paris-Sud, Université Paris-Saclay, Clamart, France

<sup>13</sup> CHU de Nîmes, Nîmes, France

<sup>14</sup> Sorbonne Université, France

<sup>16</sup> RMB-PPC, INM, Univ Montpellier, CHU Montpellier, INSERM CNRS, Montpellier, France

<sup>17</sup> Department of Medical Information (DIM), Centre Hospitalier Universitaire de Montpellier, Montpellier, France

26 <sup>18</sup> Department of Infectious and Tropical Diseases, Centre Hospitalier Universitaire de  
27 Montpellier, Montpellier, France

28 <sup>19</sup> Center for Free Information, Screening and Diagnosis (CeGIDD), Centre Hospitalier  
29 Universitaire de Montpellier, Montpellier, France

30 <sup>20</sup> German Cancer Research Center (DKFZ), Infections and Cancer Epidemiology, Heidelberg,  
31 Germany

32 <sup>21</sup> National Microbiology Laboratory (NML), Public Health Agency of Canada (PHAC),  
33 Canada

34 + equal contribution

35 \* Corresponding author: [samuel.alizon@cnrs.fr](mailto:samuel.alizon@cnrs.fr)

36 **Human papillomavirus (HPV) infections drive one in twenty new cancer cases.**  
37 **Despite the potential for improving treatment, screening, and vaccination strate-**  
38 **gies, little is known as to why most HPV infections clear spontaneously within**  
39 **two years. To untangle the dynamics of these non-persisting infections, we per-**  
40 **formed a combined quantitative analysis of virological, immunological, and**  
41 **clinical data from an original longitudinal cohort of 189 women with high**  
42 **temporal resolution. We find that HPV viral load reaches a plateau within**  
43 **two months, and clears within a median time of 14 months. Furthermore,**  
44 **we identify immune correlates associated with infection clearance, especially**  
45 **TCR-gamma-delta cells. Our results open new perspectives for understanding**  
46 **the frontier between acute and chronic infections and for controlling HPV-**  
47 **associated diseases.**

48 Human papillomaviruses (HPVs) cause nearly all cervical cancers, the majority of many anogen-  
49 ital cancers, and a significant fraction of oropharyngeal cancers (1). Women and low-medium  
50 income countries are the most affected, with respectively 90% and 65% of the 630,000 HPV-  
51 induced cancers reported in 2012 worldwide (1). This burden, further exacerbated by millions  
52 of cases of anogenital warts (2), stems from the fact that HPVs are among the most preva-  
53 lent sexually-transmitted infections (STIs), with a high transmission risk per sexual contact (3).  
54 Fortunately, more than 90% of these infections do not persist for more than two years in young  
55 adults (4–7). The factors driving infection clearance are poorly known and could involve the  
56 adaptive and the innate immune response (8), but also random events occurring during cell  
57 division (9, 10). Over the last two decades, safe and efficient vaccines have been developed  
58 that target the most oncogenic genotypes (especially HPV16 and HPV18), as well as genotypes  
59 causing genital warts (HPV6 and HPV11) (11, 12). Notwithstanding, chronic infections by  
60 HPVs will remain a major public health issue for at least one generation because of low vaccine  
61 coverage in many countries and decreased vaccine efficacy if administered after exposition (13).  
62 Non-persisting, or ‘acute’, HPV infections are often asymptomatic and benign but raise im-  
63 portant challenges (14). First, the quality of screening policies relies on the description of the  
64 natural history of the infection (15). Furthermore, understanding interactions between HPVs  
65 and the immune system may shed new light on the factors that lead to clearance or chronicity,  
66 with implications for human cancers of infectious origin (16), and the development of im-  
67 munotherapies (17). Finally, non-persisting HPV infections represent a major reservoir of virus  
68 diversity, which could fuel an evolutionary response to vaccine-driven selective pressures (18).  
69 Unfortunately, although we have known for decades about the prevalence and duration of non-  
70 persisting HPV infections (4, 5, 19), we still know little about the immune response they might  
71 elicit and temporal variations in virus loads.  
72 To address this matter, we implemented a longitudinal cohort study in Montpellier (France) dur-

73 ing which 189 women aged from 18 to 25 years old were followed every two months until HPV  
74 infection clearance or for a maximum duration of 24 months (20). At each of the 974 on-site  
75 visits, biological samples were collected and participants filled in detailed socio-demographic,  
76 health, and behaviour questionnaires. The strength of the study stems from its temporal resolu-  
77 tion and the quality of the biological data generated. The main characteristics of the cohorts are  
78 shown in Table S1 and in Ref. (21).

### 79 **Immune response to HPV infections**

80 HPV infections are poorly immunogenic and only 40 to 60% of HPV-positive women serocon-  
81 vert to an incident viral genotype (22). Therefore, we focused on the local cellular immune  
82 response and used flow cytometry (FCM) to analyse cervical smears. These biological sam-  
83 ples are particularly fragile and challenging to study because keratinocytes are highly adhe-  
84 sive and autofluorescent cells. Building on an existing protocol (23) and on existing software  
85 packages (24), we devised a pipeline to identify clusters of immune cell populations with a  
86 non-supervised approach. We first used this pipeline to identify leukocytes (CD45<sup>+</sup> cells). We  
87 then applied it to this cell population to automatically delineate 20 cellular clusters, which we  
88 could manually group into 11 distinct immune cell populations based on morphological and  
89 lineage markers (Fig. S2, S3, and Table S3). The most frequent cells were CD16<sup>+</sup> granulocytes  
90 (59.9%). We could also notably identify three distinct populations of TCR $\gamma\delta$  cells (clusters III,  
91 VII and IX), representing respectively 3.88%, 12.44%, and 0.73% of the CD45<sup>+</sup> cells (Fig S2),  
92 as well as CD4 and CD8 T cells (respectively 1.15% and 0.78%). Other cell populations could  
93 not be assigned formally but display features of local antigen-presenting cells (cluster V) or NK  
94 cells (cluster II) (Fig. S2).

95 We stratified the samples as HPV negative or positive for a ‘focal’ HPV genotype, *i.e.* a geno-  
96 type detected at least during two consecutive visits (Fig. S1 and Table S2). This emphasis was

97 made to avoid a spurious focus on ‘singletons’, *i.e.* an HPV genotype detected at a single visit.  
98 These are sometimes referred to as ‘transient infections’ (25) and are a poor marker of actual  
99 infections (26). A UMAP clustering helped visualise the 11 immune cell populations and the  
100 composition shift in samples with a focal HPV, especially an increase of cluster VII (Fig. 1A).  
101 A differential abundance analysis (Fig. 1B) confirmed that focal HPV-positive samples exhib-  
102 ited a lower proportion of cluster X (CD4<sup>+</sup> T-cells) than HPV-negative samples (Fold Change,  
103 FC: 0.62) and a higher abundance of cluster VII (CD45<sup>low</sup> TCR $\gamma\delta$  cells) and cluster VIII (FC:  
104 1.71 and 1.41, Fig. 1B and C). Clusters IV, V, and VI were also rarer in focal HPV-positive  
105 samples (FC: 0.63, 0.71, and 0.67). These differences were statistically significant in a multi-  
106 variate generalized linear mixed model including anti-HPV vaccination status as a fixed effect  
107 and a random effect accounting for the multiple sampling per participant (Fig. 1C). Differential  
108 expression analysis highlighted moderate changes for activation markers CD69 or CD161 fluo-  
109 rescence levels. We did find a reduced median signal intensity for CD69 on CD4 T cells, which  
110 suggests lower priming of CD4 T cells during focal HPV infections (cluster X, Fold change =  
111 0.90, p-adj = 0.04) (Table. S4).

112 Building on previous results showing an association with HPV infections (27), we quantified  
113 the concentrations of five cytokines in cervical secretions using Meso Scale Discovery technol-  
114 ogy and normalised the values over total protein concentration. Associations with HPV status  
115 (Fig. S4) were consistent with earlier cross-sectional studies (27, 28). To improve the character-  
116 ization of immune cells, we explored correlations between the proportion of each immune cell  
117 population in a sample and the concentration of each cytokine in the same sample (Fig. 2A).  
118 Our linear models identified positive correlations between the concentration of IFN $\gamma$  and the  
119 frequency of CD8 T cells (cluster XI,  $\beta = 0.14$ ), although with a p-value of 0.062, and to a  
120 lower extent with CD45<sup>+</sup> TCR $\gamma\delta$  cells (cluster IX,  $\beta = 0.05$ ,  $p = 0.03$ ). We also found a  
121 negative correlation between IL-17A and cluster VIII ( $\beta = -0.28$ ,  $p = 0.019$ ).

122 Combining all cervical immune variables (cytokines and immune cell populations) in a multiple  
123 factor analysis showed a trend for differential clustering of samples originating from HPV focal  
124 infections and from uninfected women (Fig. 2B). The axes indicate that HPV focal infections  
125 were negatively correlated with IFN- $\gamma$  and IL-17a concentrations and frequency of CD16<sup>+</sup> gran-  
126 ulocytes (clusters I and II) (Fig. 2C). Conversely, the main vectors associated with HPV focal  
127 infection were CD45<sup>low</sup> TCR $\gamma\delta$  cells (cluster VII) and cluster VIII (Fig. 2C).

### 128 **Viral load kinetics**

129 For all 126 participants with at least one HPV genotype detected, we estimated the virus load  
130 in all the cervical smears collected at each on-site visit for 13 HPV genotypes using a sensitive  
131 and specific quantitative Polymerase Chain Reaction (qPCR) protocol (29). The number of viral  
132 copies was normalised by that of a cellular gene (albumin). We could monitor 160 infections,  
133 including 28 complete infections (18%), 99 left-censored where participants were enrolled as  
134 positive (62%), and 69 right-censored where clearance was not observed (43%) (Fig. 3).

135 Given the longitudinal nature of our data, we turned to the field of viral kinetics (30) and de-  
136 veloped Bayesian non-linear mixed-effects models (31, 32). We described virus dynamics with  
137 five parameters capturing an increasing slope, a plateau, and a declining slope (Fig 4A and  
138 Methods). This shape was motivated by the important frequency of left- and right-censored  
139 follow-ups and the fast rate of reaching the plateau, which a simpler model with two slopes  
140 could not capture. Moreover, a similar plateau was observed to emerge in a previous mathemat-  
141 ical model of HPV dynamics in squamous epithelia (33).

142 The resulting model parameter estimates captured the per-participant variability in normalised  
143 virus load values and exhibited wider uncertainty in censored follow-ups (Fig. 3). The popu-  
144 lation average of the mixed effect model (Fig. 4B) indicated that infections lasted 14 months  
145 (95% Credibility Interval, CrI, 11 to 18), with a 12 months (95% CrI: 10 to 15) plateau at 11

146 virus genomic copies per cell (95% CrI: 5 to 21). According to the model, 90% of the infections  
147 clear within three years, which is in line with earlier studies (7).

## 148 **Immune kinetics**

149 We then used the same method but with a different model to analyse the flow cytometry (FCM)  
150 time series. We transformed the cell population proportions using centered log-ratios (34) and  
151 assumed a two-slope model with matching dates of the beginning and end of the infection to  
152 the virus load fit. At the population level, some clusters of cells exhibited similar kinetics  
153 during the course of infection (Fig. 4C). The first group consisted of clusters I and II, which we  
154 associated with the innate immune response, and increased in relative proportion after the onset  
155 of infection. Another group (clusters VII and VIII) exhibited a smaller and later peak. Finally,  
156 a third group (clusters VI, IX, X, and XI) was associated with the adaptive immune response  
157 and decreased in frequency over the course of the infection. Moreover, the frequency of the  
158 remaining clusters (III, IV, and V), which were associated with the innate immune response,  
159 tended to decline during the infection. These cells clusters groups also appear when analysing  
160 inter-individual variation through the random effects correlation matrixes inferred by the model  
161 (Fig. S7).

162 We assumed the same two-slope model for the cytokines concentration dynamics in the cervix.  
163 At the population level, CCL20 increased over the course of the infection whereas IFN $\gamma$  decreased.  
164 The other cytokines remained steady, although with an important variability between partici-  
165 pants (Fig. 4D). Analysing inter-individual variation patterns indicated that the concentrations  
166 of CCL20 and CXCL10 were closely correlated, and negatively correlated to those of IL-17A  
167 and IFN $\gamma$  (Fig. S8).

168 Finally, circulating IgG and IgM antibodies specifically targeting 10 HPV genotypes were quan-  
169 tified using a multiplex assay (21, 35). We assumed a classical Bateman function for the dy-



170 namics (36) and only considered IgG and IgM specific to the infecting HPV genotype. This  
171 limited the analysis to 55 infections in 37 individuals but still allowed us to identify a marked  
172 difference between IgG and IgM with a steeper decline of the latter (Fig. 4E).

### 173 **Linking viral dynamics and immunity**

174 We then compared the infection duration and the magnitude of the virus load with the immune  
175 response. For multiply infected individuals, we focused on the longest infection, which also  
176 generally had the highest plateau viral load (Fig. S6). Because of the compositional (and there-  
177 fore highly correlated) nature of the data, we used partial least square (PLS) regressions for the  
178 analysis.

179 The regression explained a third of the variance in infection duration ( $R_{adj.}^2 = 0.33$ ), which  
180 was found to be significantly correlated with the mean concentration of IFN $\gamma$  and the mean  
181 frequency of FCM clusters VIII and IX, but negatively associated with CXCL10 (Fig. 5A).  
182 Furthermore, HPV species  $\alpha 5$  had a significantly shorter infection duration than the reference  
183 species  $\alpha 9$  (which includes HPV16). The strong association between the multiply-infected sta-  
184 tus and the infection duration was expected since we kept the longest infection per participant in  
185 the model. Finally, for a smaller subset of participants infected by a genotype we could identify  
186 both with serology and qPCR, being seropositive in IgGs beforehand led to shorter infections  
187 (9.9 months, 95% CI: 7.7-12.8) than in seronegative individuals, even if they seroconverted  
188 (17.0 months, 95% CI: 12.0-24.1, Fig. 5B). Out of the 12 infection events where we observed  
189 the end of the infection and the individuals were initially seronegative, four never seroconverted  
190 (33%).

191 Regarding the magnitude of the plateau virus load, the proportion of the variance explained  
192 by the PLS regression was lower than for the infection duration ( $R_{adj.}^2 = 0.19$ ) (Fig. 5C) but  
193 the HPV species had a stronger impact. Indeed, compared to the reference species  $\alpha 9$ ,  $\alpha 6$

194 had a higher viral load, whereas  $\alpha 5$  had a lower one. The mean frequency of cluster VI was  
195 also negatively correlated with the plateau viral load (although only with  $p < 0.1$ ). This is  
196 consistent with this cluster most likely corresponding to B lymphocytes (our FCM analysis  
197 being supported by the observation that among women with matching IgG data, its frequency  
198 was associated with the mean IgG titers in the serum, Fig. S9). Finally, women who were  
199 seropositive before the infection had a plateau viral load on average 7.6 times smaller (95% CI:  
200 2.4-25) than those who seroconverted during the infection (Fig. 5D).

## 201 Discussion

202 While most HPV infections in young adults last less than two years (4, 6, 7, 15), HPV clear-  
203 ance processes and mechanisms remain elusive. Thanks to the combination of dense moni-  
204 toring, high-quality data, and statistical models, we offer original insights into HPV-immunity  
205 clearance dynamics.

206 HPV infections exhibit three phases: a short growth phase, a long plateau phase, and, for some  
207 of them, a short clearance phase. This is consistent with an existing mathematical model (33)  
208 and prior knowledge on infection duration. Our work is limited to studying the path to chronic  
209 infections because participants were not followed after 24 months of infection by the same  
210 HPV (only 4 of the 126 infected women did not clear the infection in 18 months). Furthermore,  
211 although dense, our follow-up has a 4 months uncertainty window around ‘singletons’, i.e. HPV  
212 detection at a unique visit. Studies with denser follow-ups are required to better understand  
213 whether these events correspond to short productive infections.

214 Given the little prior knowledge, we studied both innate and adaptive immune responses. Fo-  
215 cusing on lymphoid immunity and harnessing the power of unsupervised clustering enabled us  
216 to highlight the importance of TCR $\gamma\delta$  cells on HPV dynamics, with at least three distinct sub-  
217 populations. The dominance of TCR $\gamma\delta$  cells in mucosal immunity could explain their relative

218 abundance in our samples. This is also consistent with recent studies on cervical smears that  
219 did not include these cells in their panels but found a relatively higher abundance of T cells (37,  
220 38).

221 We also found a lower proportion of CD4 T cells (cluster X) in individuals with a focal HPV  
222 infection compared to uninfected individuals. Furthermore, a population yet to be characterised  
223 in details, cluster VIII, was more frequent in focal HPV infections and associated with longer  
224 infections. Based on its expression pattern, we hypothesise that it could contain ILCs or pro-  
225 genitors, but not ILC3 given the lack of correlation between this cluster and IL-17A (Fig. 2)  
226 (39).

227 Among the infected participants for whom we could monitor viral kinetics by qPCR, Bayesian  
228 hierarchical modelling identified a positive correlation between the infection duration and only  
229 one of the three TCR $\gamma\delta$  populations (cluster IX with CD45<sup>+</sup> TCR $\gamma\delta$  cells). This highlights the  
230 diversity of these populations and points to their different roles at specific times of the infection  
231 course (40).

232 Infection duration was also positively correlated with IFN $\gamma$  mean concentration in the cervical  
233 area, which is consistent with earlier results. Unexpectedly, longer infections were associ-  
234 ated with decreased concentrations of CXCL10, although the release of this cytokine is usually  
235 stimulated by IFN $\gamma$  (41). One interpretation is that averaging the overall response during the in-  
236 fection may buffer time-dependent patterns of the antiviral response. Another hypothesis could  
237 be that only the HPV infections that manage to evade the innate immune response can estab-  
238 lish a more persistent infection, thereby triggering the adaptive immune response. In this case,  
239 CXCL10 would only be elevated during the early immune response. This is consistent with  
240 results from a comparable cohort indicating that persistence is associated with high levels of  
241 proinflammatory, Type-1, and regulatory cytokines (25).

242 We did not observe any 'breakthrough' focal infection in the study and, as a consequence, vac-

243 cine status was not associated with infection duration or plateau viral load. We did, however,  
244 observe a trend towards shorter infections among vaccinated individuals, which could be at-  
245 tributed to a mild cross-protective mechanism. This is also consistent with our observation that  
246 participants who were seropositive for an HPV genotype before being infected by this same  
247 genotype exhibited shorter infections with lower virus loads. This shows that natural immunity  
248 may provide protection against infection but is not sufficient to prevent it. Note that this impor-  
249 tance of the serological status, which was missing for some HPV types, imposes nuancing the  
250 role of the other factors on the duration of the infection and the plateau virus load.

251 Our immunological analyses lay the ground for future work. Future extensions could be to  
252 investigate markers more related to myeloid immune cells. On the statistical side, adding a tem-  
253 poral dimension via the kinetics analyses allowed us to extract more information from the data  
254 by harnessing the longitudinal information inherent to the cohort. Future studies could build on  
255 existing within-host dynamics models to estimate more biologically-relevant parameters, such  
256 as the ‘burst size’ of infected cells or the killing rate by the immune response (33).

257 Both the vaginal microbiota (42) and the immune response vary over the course of the menstrual  
258 cycle (43) with, for instance, fewer immunoglobulins during the luteal phase and, conversely,  
259 more IL-1 $\alpha$ . Furthermore, the vaginal community state type has been associated with the risk  
260 of HPV detection (26) but investigating how menstrual cycles interact with the course of HPV  
261 infection dynamics would require denser follow-ups.

262 Cohort participants were followed for a mean duration of 290 days. Long-term follow-up of  
263 these women could yield valuable insights, especially thanks to new development in HPV full  
264 genome sequencing (44). For instance, it could help to estimate the prevalence of latent infec-  
265 tions (45) but also further monitor the dynamics of chronic infections (46). Finally, it would  
266 provide critical data on HPV within-host evolution, which could be associated with cancer de-  
267 velopment since HPV16 found in cervical cancers has a particular genomic signature with less

268 variation in the E7 gene (47).

269 Beyond the case of HPVs, this system represents an opportunity to better understand the some-  
270 times tenuous frontier between non-persisting and chronic viral infections (48).

## 271 **References**

- 272 1. C. de Martel, M. Plummer, J. Vignat, S. Franceschi, *Int J Cancer* **141**, 664–670 (2017).
- 273 2. D. Forman *et al.*, *Vaccine* **30**, F12–F23 (2012).
- 274 3. R. L. Winer *et al.*, *N Engl J Med* **354**, 2645–54 (2006).
- 275 4. G. Y. Ho, R. Bierman, L. Beardsley, C. J. Chang, R. D. Burk, *N Engl J Med* **338**, 423–  
276 428 (1998).
- 277 5. A.-B. Moscicki *et al.*, *J Pediatr* **132**, 277–284 (1998).
- 278 6. R. P. Insinga, E. J. Dasbach, E. H. Elbasha, K.-L. Liaw, E. Barr, *Cancer Epidemiol*  
279 *Biomarkers Prev* **16**, 709–15 (2007).
- 280 7. A. V. Ramanakumar *et al.*, *BMJ Open* **6**, e011371 (2016).
- 281 8. M. Stanley, *Current Opinion in Virology* **51**, 106–110 (2021).
- 282 9. M. D. Ryser, E. R. Myers, R. Durrett, *PLoS Comput Biol* **11**, e1004113 (2015).
- 283 10. T. Beneteau, C. Selinger, M. T. Sofonea, S. Alizon, *PLoS Comput Biol* **17**, e1009352  
284 (2021).
- 285 11. R. Herrero, P. González, L. E. Markowitz, *Lancet Oncol* **16**, e206–16 (2015).
- 286 12. J. Lei *et al.*, *New Engl J Med* **383**, 1340–1348 (2020).
- 287 13. L. Bruni *et al.*, *Lancet Glob Health* **4**, e453–63 (2016).
- 288 14. S. Alizon, C. L. Murall, I. G. Bravo, *Viruses* **9**, 293 (2017).
- 289 15. M. Schiffman, D. Solomon, *N Engl J Med* **369**, 2324–31 (2013).
- 290 16. C. P. Wild, Weiderpass, B. W. Stewart, Eds., *The World Cancer Report* (International  
291 Agency for Research on Cancer, Lyon, France, 2020).
- 292 17. J. G. Skeate, A. W. Woodham, M. H. Einstein, D. M. D. Silva, W. M. Kast, *Hum Vaccin*  
293 *Immunother* **12**, 1418–1429 (2016).
- 294 18. C. L. Murall, C. T. Bauch, T. Day, *Proc B* **282**, 20141069 (2015).
- 295 19. C. B. Woodman *et al.*, *The Lancet* **357**, 1831–1836 (June 2001).
- 296 20. C. L. Murall *et al.*, *BMJ Open* **9**, e025129 (2019).
- 297 21. C. L. Murall *et al.*, *Vaccine* **38**, 8167–8174 (2020).
- 298 22. M. Mollers *et al.*, *J Med Virol* **85**, 1379–1385 (2013).
- 299 23. J. A. Juno, G. Boily-Larouche, J. Lajoie, K. R. Fowke, *J Vis Exp* **89**, e51906 (2014).
- 300 24. L. M. Weber, M. Nowicka, C. Sonesson, M. D. Robinson, *Commun Biol* **2**, 183 (2019).
- 301 25. M. E. Scott *et al.*, *International Journal of Cancer* **133**, 1187–1196 (2013).
- 302 26. R. M. Brotman *et al.*, *J Infect Dis* **210**, 1723–33 (2014).

- 303 27. C. Selinger *et al.*, *Immunol Res* **69**, 255–263 (2021).
- 304 28. L. J. P. Liebenberg *et al.*, *Nature Communications* **10**, 5227 (2019).
- 305 29. I. M. Micalessi, G. A. V. Boulet, J. J. Bogers, I. H. Benoy, C. E. Depuydt, *Clin Chem*  
306 *Lab Med* **50**, 655–661 (2012).
- 307 30. L. Canini, A. S. Perelson, *J Pharmacokinet Pharmacodyn* **41**, 431–443 (2014).
- 308 31. E. Comets, A. Lavenu, M. Lavielle, *J Stat Software* **80**, 1–41 (2017).
- 309 32. S. M. Kissler *et al.*, *New Engl J Med* **385**, 2489–2491 (2021).
- 310 33. C. L. Murall *et al.*, *PLoS Comput Biol* **15**, e1006646 (2019).
- 311 34. J. Aitchison, *Lecture Notes-Monograph Series* **24**, 73–81 (1994).
- 312 35. T. Waterboer *et al.*, *Clin Chem* **51**, 1845–1853 (2005).
- 313 36. E. R. Garrett, *J. Pharmacokinet. Biopharm.* **22**, 103–128 (1994).
- 314 37. B. Shannon *et al.*, *Mucosal Immunology* **10**, 1310–1319, ISSN: 1935-3456 (2017).
- 315 38. A. M. Zaki *et al.*, *Front. Microbiol.* **13** (June 2022).
- 316 39. M. D. Hazenberg, H. Spits, *Blood* **124**, 700–709 (2014).
- 317 40. D. Van hede *et al.*, *Proc Nat Acad Sci USA* **114** (2017).
- 318 41. A. D. Luster, J. C. Unkeless, J. V. Ravetch, *Nature* **315**, 672–676 (1985).
- 319 42. P. Gajer *et al.*, *Sci Transl Med* **4**, 132ra52 (2012).
- 320 43. S. M. Hughes *et al.*, *BMC Med* **20**, 353 (2022).
- 321 44. A. Holmes *et al.*, *Genomic Med* **1**, 1–16 (2016).
- 322 45. P. E. Gravitt, *J Clin Invest* **121**, 4593–4599 (2011).
- 323 46. C. E. Depuydt *et al.*, *Cancer Med* **4**, 1294–1302 (2015).
- 324 47. L. Mirabello *et al.*, *Cell* **170**, 1164–1174.e6 (2017).
- 325 48. H. W. Virgin, E. J. Wherry, R. Ahmed, *Cell* **138**, 30–50 (2009).

## 326 **Acknowledgments**

327 This project has received funding from the European Research Council (ERC) under the Euro-  
328 pean Union's Horizon 2020 research and innovation programme (grant agreement No 648963,  
329 to SA).

330 The authors acknowledge further support from the Centre National de la Recherche Scien-  
331 tifique, the Institut de Recherche pour le Développement, the Fédération Hospitalière Universi-  
332 taire InCH of Montpellier, the Fondation pour la Recherche Médicale (to TK), the Ligue contre  
333 le Cancer (to TB), and the Agence Nationale de la Recherche contre le Sida (ANRS-MIE, to  
334 NT and OS).

335 The authors acknowledge the ISO 9001 certified IRD i-Trop HPC (member of the South Green  
336 Platform) at IRD Montpellier for providing HPC resources that have contributed to the research  
337 results reported within this article ([bioinfo.ird.fr](https://bioinfo.ird.fr) and [www.southgreen.fr](https://www.southgreen.fr)).

338 The raw data and R scripts used will be deposited on the Zenodo server upon publication.

## 339 **Supplementary materials**

340 Materials and Methods

341 Supplementary Results

342 Figures S1 to S9

343 Tables S1 to S9

344 References (S1-S17)

345 Ethics, competing interests, and authors' contributions



## 346 **Figures captions**

Figure 1: **Unsupervised clustering of flow cytometry data from cervical smears.** A) Highlighting 11 homogeneous populations using UMAP clustering on data from samples without HPV or positive for a ‘focal’ HPV infection, B) Comparison of the clusters frequencies based on infection status, and C) Cluster annotation and fold change (FC) values shown in panels A and B. FC were calculated by an abundance analysis with diffcyt-DA-edgeR adjusted with a Benjamini-Hochberg test.

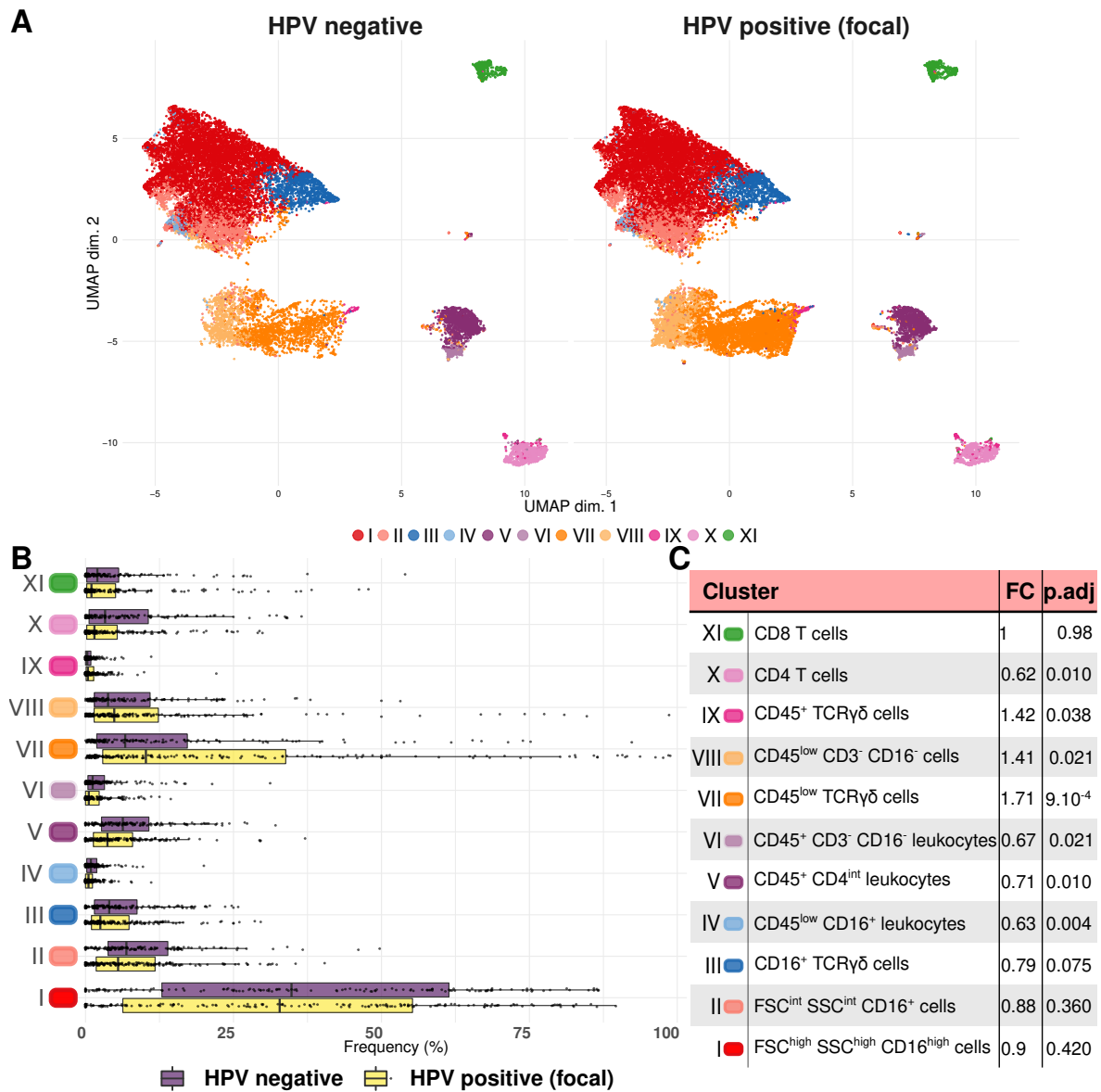
Figure 2: **Local immune response in HPV-infected and uninfected women.** A) Correlation matrix between the local density of five cytokines and the proportion of the 11 cell clusters from Figure 1. B) Sample clustering based on focal HPV infection status. C) Axes of a multiple factor analysis based on FCM and cervical cytokines and chemokines. In A, colors indicate the coefficient of pairwise regressions (only p-values lower than 10% are shown).

Figure 3: **Virus load kinetics for 160 HPV genital infections in 75 women.** Each panel corresponds to one participant and shows the number of HPV genome copies per number of human genome copies resulting from a three-slopes hierarchical Bayesian model. The lines show the posterior median trajectory and shaded area the 95% credibility interval. Open circles indicate values below the limit of detection. The letter before the anonymity number (above each panel) indicates whether the participant was vaccinated (V) or not (N).

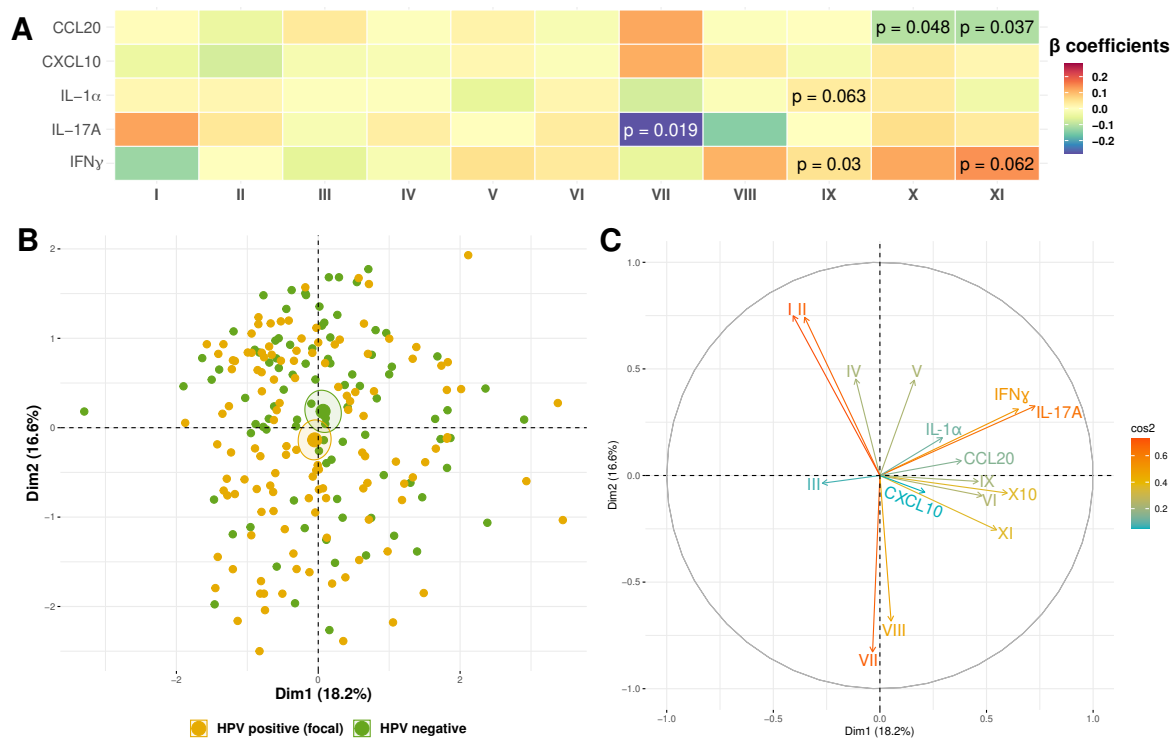
**Figure 4: Population predictions of virus and immune kinetics in HPV infections.** A) Representation of the parameters governing the descriptive models. The viral kinetics model is governed by five parameters: plateau virus load  $\psi_d$ , time to the midpoint of the infection  $t_{\text{mid}}$ , growth phase duration  $\psi_a$ , plateau duration  $\psi_b$ , and clearance phase duration  $\psi_c$ . B) Population prediction of virus load dynamics. As in all the panels, the black thick line shows the median trajectory, the shaded area the 95% highest posterior distribution, each dot represents an observation, and thin lines show observed trajectories of individual infections. C) Population prediction for immune cell dynamics in HPV infections. Cell proportions are transformed with a centered log-ratio. D) Population prediction for cytokines dynamics in HPV infections. In panels C and D, time is normalized between 0 (infection) and 1 (clearance). E) Prediction of IgG (light green) and IgM (dark green) kinetics before and during HPV infections. MFI stands for mean fluorescence intensity.

**Figure 5: Factors associated with HPV infection duration and plateau viral load.** A) Outcome of partial least squares (PLS) regressions between the infection duration and the immune response summary statistics ( $R_{adj}^2 = 0.33$ ), and B) between the viral load during the plateau and the immune response summary statistics ( $R_{adj}^2 = 0.19$ ). Variables with a 95% CI different from 0 are shown in brighter colors (yellow for a positive correlation and purple for a negative one). The HPV reference species is  $\alpha 9$ , which includes HPV16. C) Association between the inferred timing of seropositivation on infection duration and D) plateau virus load. This timing has a significant effect on the infection duration ( $F[2, 37] = 4.3, p = 0.023$ ) and on the plateau viral load ( $F[2, 41] = 7.6, p = 1.5 \cdot 10^{-3}$ ). Colors indicate vaccination status and shapes the genotype status (*i.e.* HPV16 or HPV18).

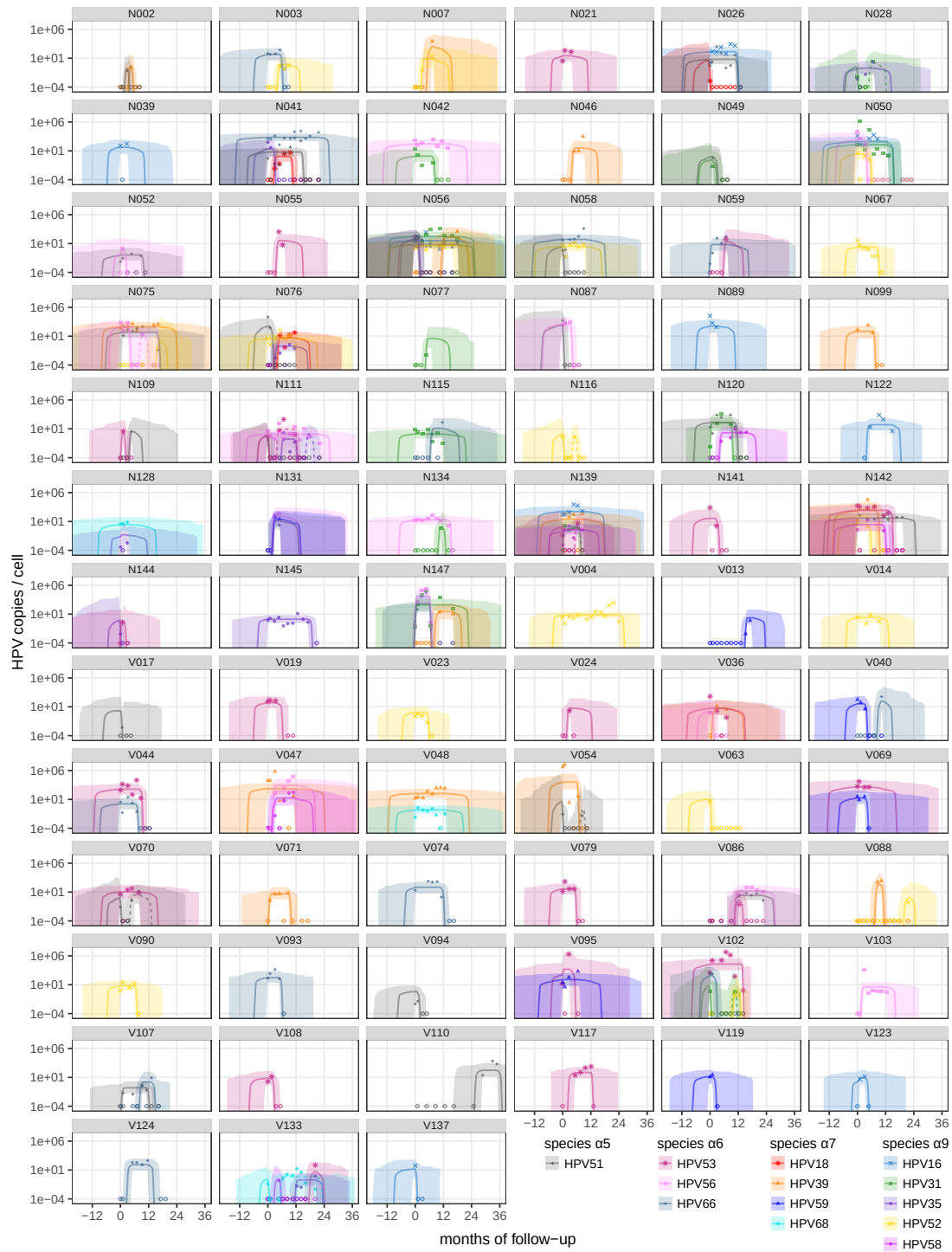
347 **Figure 1**



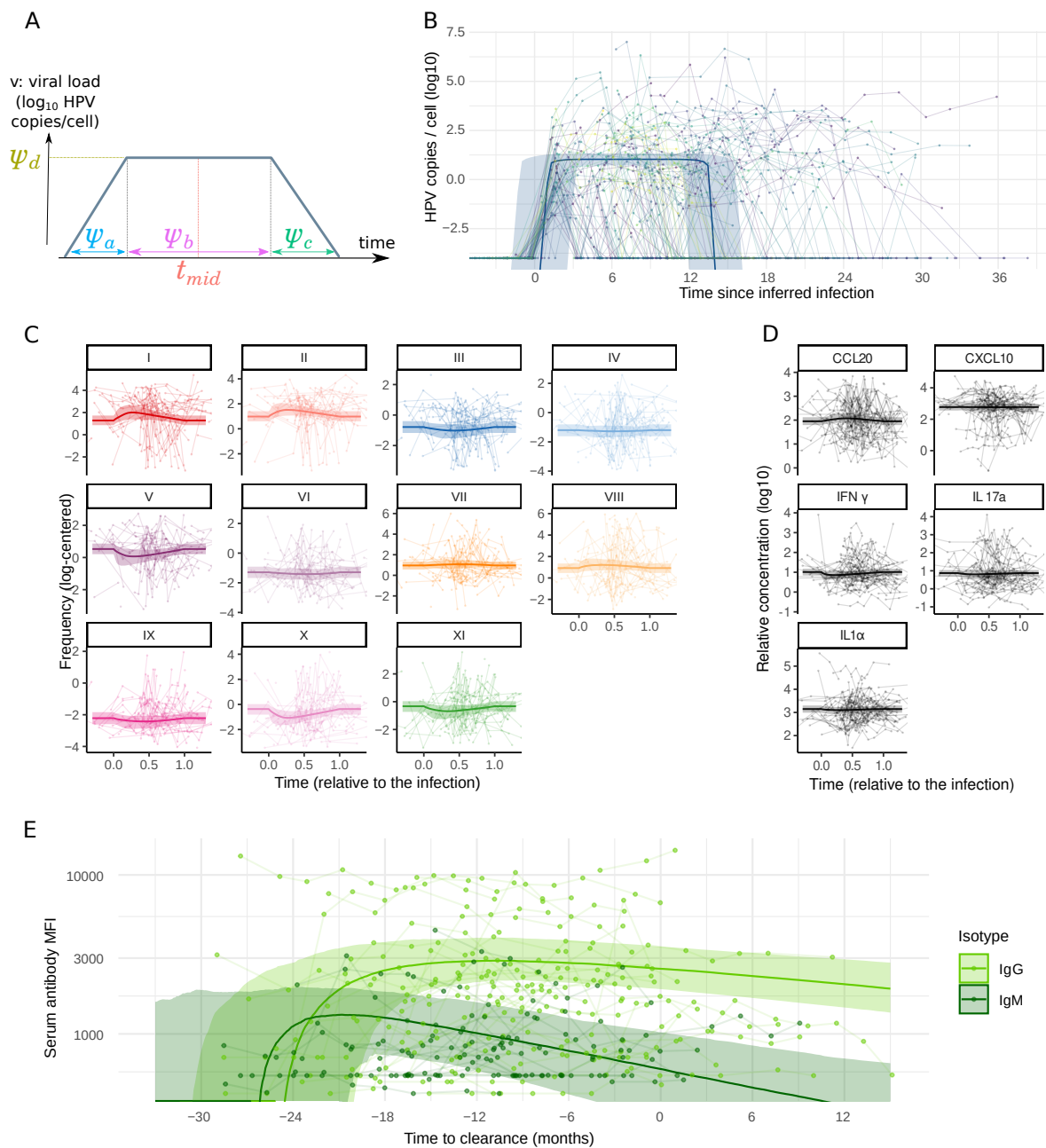
348 **Figure 2**



349 **Figure 3**



350 **Figure 4**



351 **Figure 5**

